

Enhanced Interlayer Coupling of CuO_2 Planes Promote the Superconducting Properties of $\text{Cu}_{0.5}\text{Tl}_{0.5}\text{Ba}_{2-y}\text{Sr}_y\text{Ca}_2\text{Cu}_3\text{O}_{10-\delta}$ ($Y=0, 0.15, 0.25$) Samples

Muzaffar MU^{1*}, Khan NA², Rehman UU² and Ali SA³

¹PMAS Arid Agriculture University Attock Campus, Pakistan

²Materials Science Laboratory, Quaid-i-Azam University, Islamabad, Pakistan

³Department of Physics, Government College, University Lahore, Pakistan

Abstract

The Cu-Tl-1223 superconducting samples, doping the Sr atom at Ba site, have been synthesized at 860°C pressure. The charge reservoir layer (CRL) of $\text{Cu}_{0.5}\text{Tl}_{0.5}$ -1223 superconductor is modified by doping Sr atom. The decrease in c-axis length which is most probably due to smaller size of Sr atom as compared to Ba. The substitution of Sr atom at Ba is confirmed by the Fourier Transform Infrared Spectroscopy (FTIR). The critical temperatures i.e., $T_c(R=0)$, T_c^{onset} are increased with the Sr content which shows that superconducting magnitude enhanced. The excess conductivity analysis has been done using Aslamazov-Larkin and Lawrence-Doniach models. The crossover temperatures i.e., TCR-3D=TG , T3D-2D and T2D-SWF and c-axis coherence length $\xi_c(0)$ are slanted to lower values. Moreover, the inter-plane coupling (J) increases due to decrease in c-axis length. From fluctuations induced conductivity, it is found that there is an inverse relationship between critical temperatures and coherence length.

Keywords: $\text{Cu}_{0.5}\text{Tl}_{0.5}$ -1223; Synthesis; Sr substitution; X-ray diffraction; Excess conductivity

Introduction

The cup-rate intrinsic superconducting parameters are structure dependent. There are two parts i.e., i) MBa_2O [M=Cu, Tl, Bi, Hg, C] a charge reservoir layer (CRL) and ii) conducting copper oxide planes $n\text{CuO}_2$ [1] of general unit cell in HTSC. In unit cell, the CRL provides the carriers (cooper pairs) to the cooper oxide planes and due to these carriers superconductivity exit [2-4].

Hence, the modification in CRL has a vital role in superconducting properties. In order to enhance the magnitude of superconductivity, numerous scientists have tried to modification in CRL [Co, Fe, Al] [5-7] and in CuO_2 planes [Zn, Ni] [8-10]. The increase in anisotropy and reduce in inter-plane coupling may be possible due to thicker CRL. Although, in periodic table, both atoms i.e., Sr and Ba lie in the same group but Sr atom is smaller in ionic radius (1.12 Å) as compared to Ba (1.35 Å). It is expected that dopant Sr atom would help to squeeze the CRL for enhanced interlayer coupling and hence improved the efficiency of CRL to the conducting CuO_2 planes. In contrast to the fixed Cu valence (~2+) in the Tl-bilayer cuprate superconductors, the average formal valence of Cu in the Tl-monolayer compounds $\text{TlBa}_2\text{Ca}_{n-1}\text{Cu}_n\text{O}_{2n+3}$ varies as $(2+n-1)+$. This characteristic is reflected in linear augmented-plane-wave band-structure results for the simplest $n=1$ member of this Tl-monolayer homologous series, $\text{TlBa}_2\text{CuO}_5$, where the filling (~0.16) of the planar $\text{Cu}(3d)\text{-O}(2p)$ σ^* band is reduced well below one-half. It is shown that the 50-50 Ba-La alloy is an appropriate “parent” compound for this $n=1$ phase since the half-filled-band condition is restored. For any member of this Tl-monolayer series, the optimal doping for high-temperature superconductivity should involve a combination of structural and chemical contributions.

Experimental Details

Synthesis

The superconducting samples $\text{Cu}_{0.5}\text{Tl}_{0.5}\text{Ba}_{2-y}\text{Sr}_y\text{Ca}_2\text{Cu}_3\text{O}_{10-\delta}$ ($y=0, 0.15, 0.25$) were synthesized by using the solid state reaction method. In first step, we prepared the $\text{Cu}_{0.5}\text{Ba}_{2-y}\text{Sr}_y\text{Ca}_2\text{Cu}_3\text{O}_{10-\delta}$ ($y=0, 0.15, 0.25$) by mixing the $\text{Ca}(\text{NO}_3)_2 \cdot 4\text{H}_2\text{O}$, $\text{Cu}(\text{CN})_2$, SrCO_3 and $\text{Ba}(\text{NO}_3)_2$ as starting

compounds. These compounds were thoroughly mixed for almost 2 hours in mortar and pestle. The chamber furnace at 860°C is used for heat treatment. After 24 hours continuously firing, the furnace was put off. Repeat the process under the same atmosphere.

In second step, well calculated amount of thallium oxide (Tl_2O_3) was added in precursor material and thoroughly mixed. The material was pelletized and these pellets were sintered for nearly 10 min to get finally $\text{Cu}_{0.5}\text{Tl}_{0.5}\text{Ba}_{2-y}\text{Sr}_y\text{Ca}_2\text{Cu}_3\text{O}_{10-\delta}$ ($y=0, 0.15, 0.25$) samples.

Characterizations

To measure the resistivity, we used four-probe method was used. In this method, four uniformly spaced silver paste contacts were applied. The crystal structure of the material was determined by X-ray diffraction (XRD) measurements using Bruker diffractometer at X-ray wavelength of 1.5418 Å.

Results and Discussion

The crystal structure of $\text{Cu}_{0.5}\text{Tl}_{0.5}(\text{Ba}_{2-y}\text{Sr}_y)\text{Ca}_2\text{Cu}_3\text{O}_{10-\delta}$ where; $y=0, 0.15$ and 0.25 superconducting samples have been determined from the x-ray diffraction data, shown in Figure 1. The dimensions of unit cell were calculated from check cell. All the samples have orthorhombic structure with Pmmm space group. It can be seen from Figure 1 that there is a slight shift in peak positions to higher 2 theta values with the increase of Sr content, which is most probably due to the decrease in the c-axis length of the unit cell. The overall contraction of the unit cell can be seen from the decrease of both a and c axis with the Sr content

*Corresponding author: PMAS Arid Agriculture University Attock Campus, Pakistan, Tel: 920519292122; E-mail: m.usman@uaar.edu.pk

Received August 11, 2016; Accepted November 10, 2016; Published November 20, 2016

Citation: Muzaffar MU, Khan NA, Rehman UU, Ali SA (2016) Enhanced Interlayer Coupling of CuO_2 Planes Promote the Superconducting Properties of $\text{Cu}_{0.5}\text{Tl}_{0.5}\text{Ba}_{2-y}\text{Sr}_y\text{Ca}_2\text{Cu}_3\text{O}_{10-\delta}$ ($Y=0, 0.15, 0.25$) Samples. J Material Sci Eng 5: 298. doi: 10.4172/2169-0022.1000298

Copyright: © 2016 Muzaffar MU, et al. This is an open-access article distributed under the terms of the Creative Commons Attribution License, which permits unrestricted use, distribution, and reproduction in any medium, provided the original author and source are credited.

(Figures 2a and 2b). Due to smaller in size, Sr atom prompt such modifications in the unit cell.

The resistivity versus temperature measurements of $\text{Cu}_{0.5}\text{Tl}_{0.5}(\text{Ba}_{2-y}\text{Sr}_y)\text{Ca}_2\text{Cu}_3\text{O}_{10-\delta}$ ($y=0, 0.15, 0.25$) superconducting samples are in Figure 3a and inset is shown the variation of $\rho_{290\text{K}}(\Omega\text{-cm})$ versus Sr content. These samples have shown metallic behaviour from room temperature down to onset of superconductivity. From resistivity analysis, it is observed that these samples have shown $T_c(\text{onset})$ around 114.5, 116.3 and 116.3 K whereas $T_c(R=0)$ at 90.26, 95.47 and 96.5 K respectively, shown in Figure 3b. The systematic increase of $T_c(R=0)$ and with increasing Sr content is mostly suggested that the dopant Sr atom at Ba site in $T_c(\text{onset})$ $\text{Cu}_{0.5}\text{Tl}_{0.5}\text{Ba}_{2-y}\text{O}_{10-\delta}$ (CRL) promotes efficient transfer of the carriers to the conducting CuO_2 planes and hence as a result, the aforementioned superconducting parameters enhanced. The room temperature resistivity $\rho_{290\text{K}}(\Omega\text{-cm})$ is systematically decreased with the Sr content which shows that dopant atom boosts an extra metallic trend in the final compound.

FTIR absorption measurements of $\text{Cu}_{0.5}\text{Tl}_{0.5}\text{Ba}_{2-y}\text{Sr}_y\text{Ca}_2\text{Cu}_3\text{O}_{10-\delta}$ ($y=0, 0.15, 0.25$) samples are shown in Figure 4. Three vibrational modes are witnessed around 613.4, 483.7 and 421.2 cm^{-1} in un-doped sample. However, with Sr doping in CRL, the former two modes are related to apical oxygen atoms of nature $\text{Tl-O}_A\text{-Cu}_{(2)}$, $\text{Cu}_{(1)}\text{-O}_A\text{-Cu}_{(2)}$ are softened from 483.7 to 482.0 cm^{-1} and 421.2 to 415.1 cm^{-1} whereas the third mode related to the planar oxygen atoms of nature $\text{Tl-O}_p\text{-Cu}_{(2)}$, are hardened from 613.4 to 623.4 cm^{-1} . The softening/hardening of the oxygen modes are most possibly related with the relaxation and compression of apical and planar bond lengths due to stresses and strains created after the doping of Sr atom at Ba site.

Excess conductivity analysis (FIC) $\text{Cu}_{0.5}\text{Tl}_{0.5}\text{Ba}_{2-y}\text{Sr}_y\text{Ca}_2\text{Cu}_3\text{O}_{10-\delta}$ ($y=0, 0.15$ and 0.25) samples

By fitting the experimental data of resistivity in theoretical models i.e., Aslamazov-Larkin and Lawrence-Doniach, the excess conductivity analyses is done in the temperature regime around T_c and beyond. According to Aslamzov Larkin (AL) model, the conductivity $\Delta\sigma(T)$ is given by:

$$\Delta\sigma_{AL}=C \quad (1)$$

$$\Delta[\sigma_{AL}]^{3D}=C^{3D} \quad -0.5 \quad (2)$$

$$\Delta[\sigma_{AL}]^{2D}=C^{2D} \quad -1.0 \quad (3)$$

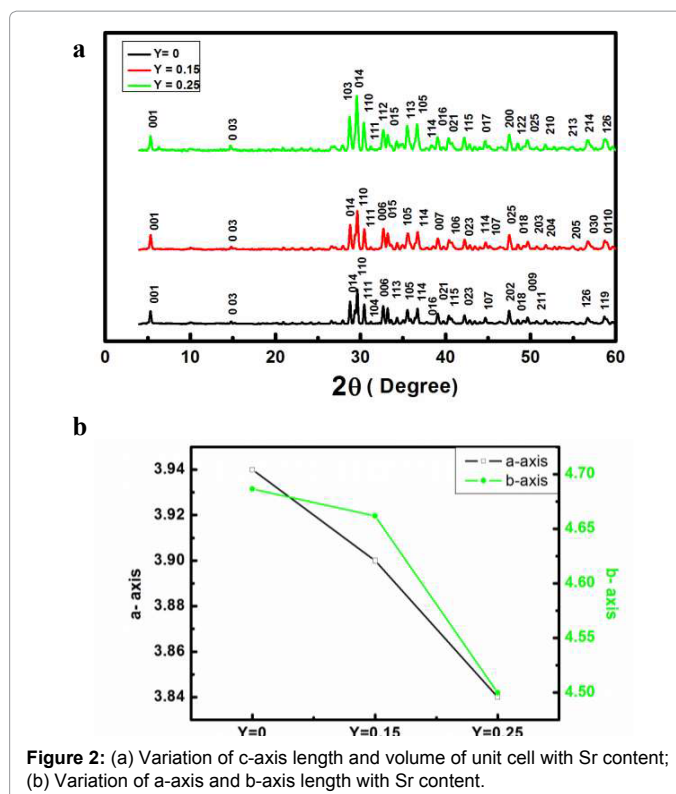
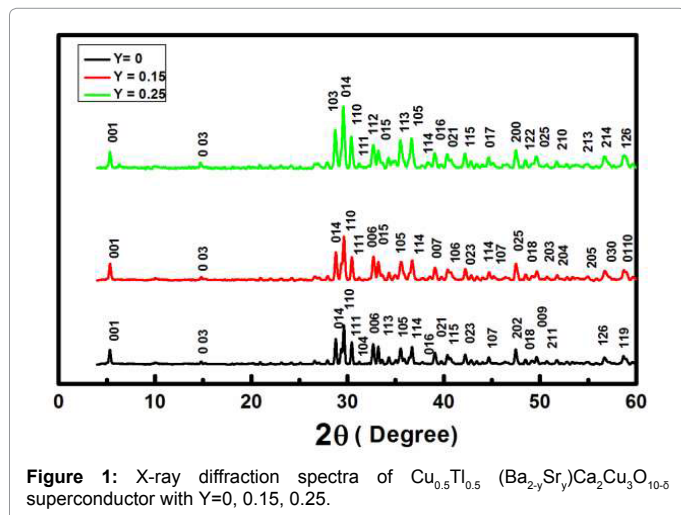


Figure 2: (a) Variation of c-axis length and volume of unit cell with Sr content; (b) Variation of a-axis and b-axis length with Sr content.

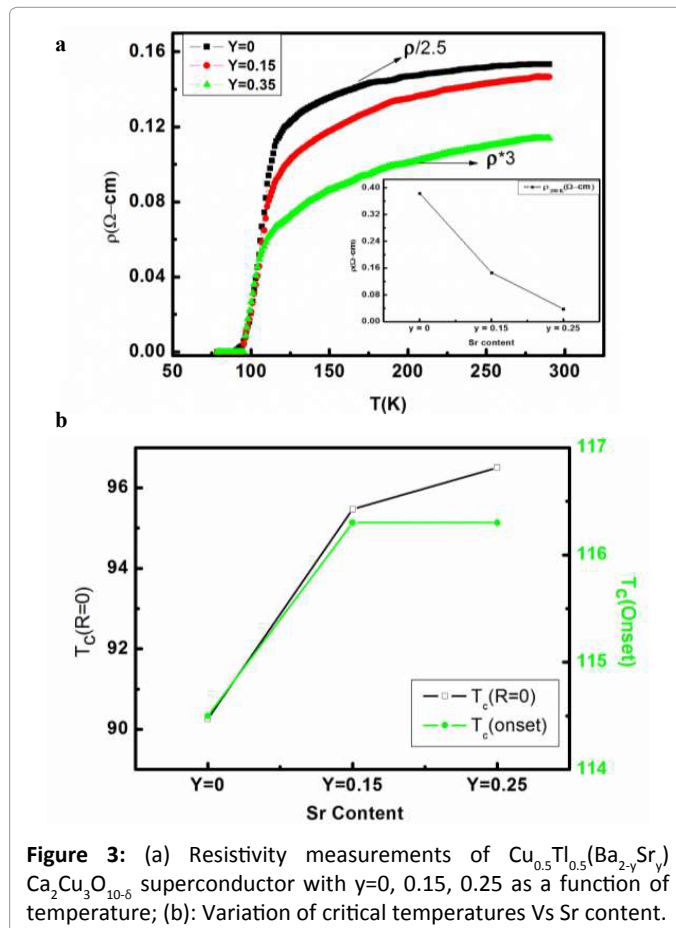


Figure 3: (a) Resistivity measurements of $\text{Cu}_{0.5}\text{Tl}_{0.5}(\text{Ba}_{2-y}\text{Sr}_y)\text{Ca}_2\text{Cu}_3\text{O}_{10-\delta}$ superconductor with $y=0, 0.15, 0.25$ as a function of temperature; (b): Variation of critical temperatures Vs Sr content.

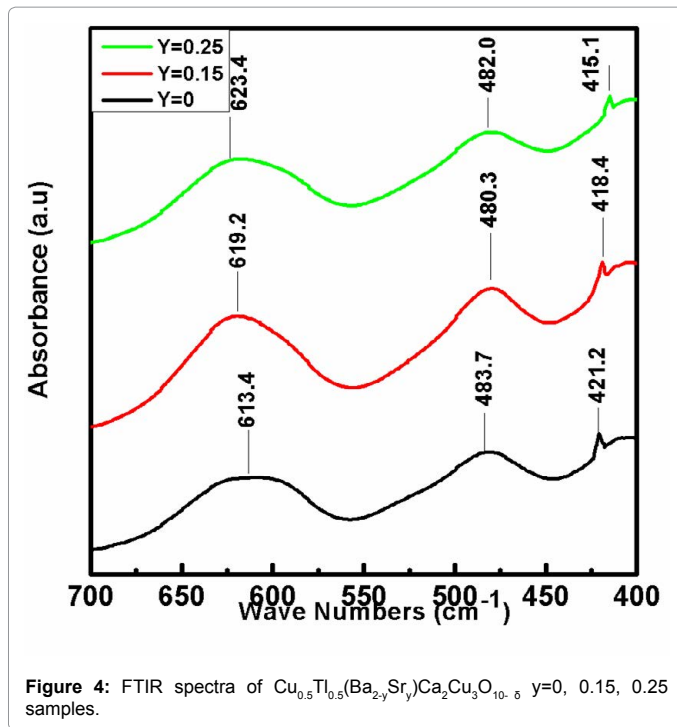


Figure 4: FTIR spectra of Cu_{0.5}Tl_{0.5}(Ba_{2-y}Sr_y)Ca₂Cu₃O_{10-δ} y=0, 0.15, 0.25 samples.

Where, C is dimensional exponent and its values vary with dimension of fluctuations i.e., 0.5, 1, 2 for 3D, 2D and 0D fluctuations respectively [11-13].

Moreover, $\frac{T_c T_{mf}}{T_c}$ is the reduced temperature, T_c is usually referred as mean field critical temperature [14,15] and C is the fluctuation amplitude.

$$C^{3D} = \frac{e^2}{32h\xi_c(0)} \quad (3)$$

$$C^{2D} = \frac{e^2}{16hd} \quad (4)$$

Where, e, d and $\xi_c(0)$ are electronic charge, inter-layer thickness and $\xi_c(0)$ coherence length respectively. Since Lowerence Donich is a modified form of Aslamsov- Larkin theory and it explained the fluctuations from 2D to 3D regimes. In the light of Lowerence Donich (LD model), the excess conductivity and cross over temperature is given below,

$$\Delta\sigma LD = A^* \epsilon^{-1} \{1 + [2\xi_c(0)/d]^2\} \quad (5)$$

$$T_{3D-2D} = T_{cmf} \{1 + [2\xi_c(0)/d]^2\} \quad (6)$$

The other parameters are given below, can be calculated by using TG and NG equations and GL theory.

$$N_G \left| \frac{T_G T_{mf}}{T_{mf}} \right| = 0.5 [K_B T_c / B_{c(0)}^2 Y^2 \xi_{c(0)}^3]^2 \quad (7)$$

$$B_{c1} = \frac{B_c}{\sqrt{2}} \ln \quad (8)$$

$$B_{c2} = \sqrt{2} B_c \quad (9)$$

$$\frac{3 \times p.d(0)}{8k_B T_0} \quad (10)$$

$$\frac{3 \times p.d(0)}{8k_B T_0} \quad (11)$$

$$V_F = \frac{5k_B T_{c(0)}}{2K} \quad (12)$$

$$E = \frac{h}{(1.6 \times 10^{19})(eV)} \quad (13)$$

The 2nd term, J i.e., Inter layer coupling is related with $J = \epsilon/4$ [16-18] here ϵ is reduced temperature. Excess conductivity $\Delta\sigma$ is determined by the expression:

$$\Delta\sigma = \rho n - \rho / \rho n^* \rho \quad (14)$$

Where, ρ is the resistivity measured experimentally and ρn is the extra-plotted normal state resistivity. The fluctuation induced conductivity analysis (FIC) has been done employing the above cited models (Aslamazov-Larkin and Lawrance-Donaich). The extracted superconducting parameters are given in Tables 1 and 2. The graphs are plotted between $\ln(\Delta\sigma)$ and $\ln(\epsilon)$ of Cu_{0.5}Tl_{0.5}Ba_{2-y}Sr_yCa₂Cu₃O_{10-δ} (y=0, 0.15, 0.25) samples are shown in Figures 5a-5c. It can be seen from Table 1 that all the crossover temperatures i.e., T_{CR-3D}, T_{3D-2D}, T_{2D-SW} have been suppressed with the Sr doping which shows that there is an inverse correlation between the crossover temperatures and superconductivity transition temperatures (T_{c0} and T_{c^{onset}}). The zero temperature coherence length, interlayer coupling strength, electron-phonon coupling parameter and critical magnetic field calculated from the excess conductivity analysis are given in Table 2. It is observed that the interlayer coupling strength has been increased with the increase of Sr in the charge reservoir layer (CRL).

The values of parameters such as B_{c0}(T), B_{c1}(T), and J_{c(0)} are increased with the Sr content. These parameters appreciably dependent on thermodynamic critical magnetic field B_c and it is related to the free energy difference at the interface of normal and superconducting electrons. So in our case, the dopant atom seems to support in the difference of free energy and as a result, these parameters increases. The coherence length along the c-axis $\xi_c(0)$ and the Fermi velocity vF of superconducting carriers are decreased with Sr content in Cu_{0.5}Tl_{0.5}(Ba_{2-y}Sr_y)Ca₂Cu₃O₁₀ unit cell. Since $K_F = (32N/V)1/3$; $[n=N/V]$, $\xi_c = \hbar 2K_F / 2m\Delta$ and V_F. These parameters are dependent on density of carriers and doping of Sr atom, increases the density of carriers which suppresses the order parameter's values. It confirms that Sr atom promote the efficiency of transfer the charge carriers to the CuO₂ planes.

Conclusion

The present work has been resulted in the following conclusions as stated by the above study. Using solid state reaction method, the Sr-doped Cu_{0.5}Tl_{0.5}1223 (y=0, 0.15, 0.25) samples were synthesized at ambient pressure. The XRD analysis shows that samples have orthorhombic crystal structure. The fluctuation induced conductivity analysis (FIC) has been done employing the above cited models (Aslamazov-Larkin and Lawrance-Donaich). Three vibrational modes are witnessed around 613.4, 483.7 and 421.2 cm⁻¹ in un-doped sample. However, with Sr doping in CRL, the former two modes are related to apical oxygen atoms of nature Tl-O_A-Cu₍₂₎, Cu₍₁₎-O_A-Cu₍₂₎ are softened from 483.7 to 482.0 cm⁻¹ and 421.2 to 415.1 cm⁻¹ whereas the third mode related to the planar oxygen atoms of nature Tl-O_P-Cu₍₂₎, are hardened from 613.4 to 623.4 cm⁻¹. The substitution of Sr at Ba site in the charge reservoir layer decreases the lattice parameters including c-axis, as a result, promotes the enhanced interlayer coupling. The magnitude of the superconductivity is notably increased with the inclusion of Sr which shows that dopant Sr atom at Ba site in Cu_{0.5}Tl_{0.5}Ba₂O₁₀ (CRL) promotes efficiency of transfer the carriers to the conducting CuO₂ planes.

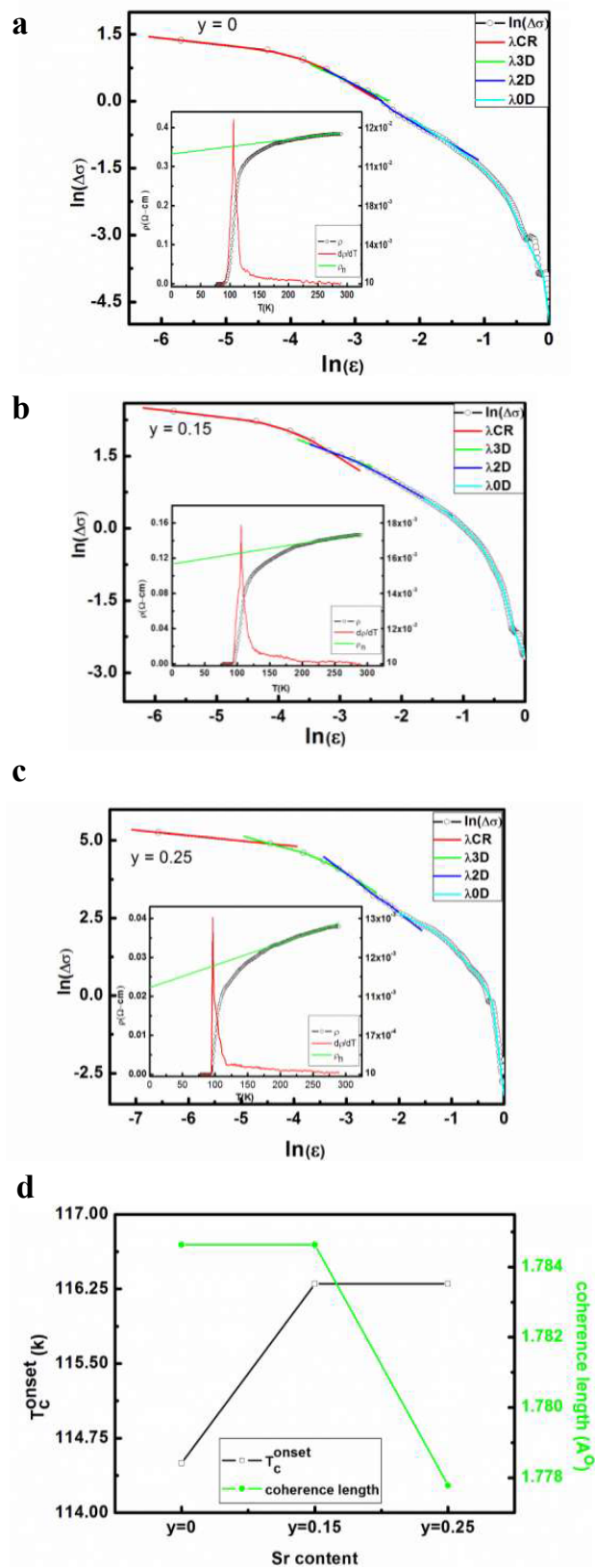


Figure 5: Representative figure of the excess conductivity analysis of $\text{Cu}_{0.5}\text{Tl}_{0.5}(\text{Ba}_{2-y}\text{Sr}_y)\text{Ca}_2\text{Cu}_3\text{O}_{10-\delta}$ ($y=0, 0.15, 0.25$) superconductors.

Sample	λCR	λ3D	λ2D	λSW	TCR-3D =TG	T3D-2D	T2D-SW	Tcmf
					(K)	(K)	(K)	(K)
Y=0	0.32	0.66	0.97	2.09	110.38	111.38	126.0	106.1
Y=0.15	0.30	0.49	0.96	2.1	110.38	111.38	125.0	106.1
Y=0.25	0.29	0.64	1.1	2.01	98.80	102.0	109.8	97.2

Table 1: Widths of critical, 3D, 2D and 0D fluctuation regions observed from fitting of the experimental data of Cu_{0.5}Tl_{0.5}Ba_{2-y}Sr_yCa₂Cu₃O_{10-δ} (y=0, 0.15, 0.25).

Sample	ξc(0) (Å)	J	NG	λp.d (Å)	Bc(0) (T)	Bc1 (T)	Bc2 (T)	κ	Jc(0)*10 ³ (A/cm ²)	VF*10 ⁷ (m/s)
Y=0	1.78	0.049	0.22	1020.6	1.426	0.06	128.7	63.79	0.76	1.47
Y=0.15	1.78	0.049	0.15	907.97	1.603	0.08	128.7	56.74	0.96	1.45
Y=0.25	1.77	0.051	0.02	561.22	2.594	0.18	128.7	35.07	2.51	1.37

Table 2: Superconductivity parameters calculated from FIC analysis of Cu_{0.5}Tl_{0.5}Ba_{2-y}Sr_yCa₂Cu₃O_{10-δ} (y=0, 0.15, 0.25).

From FTIR analysis, it has been observed that the planar and apical phonon modes are hardening and softening respectively. The library of FTIR spectra available in this laboratory includes more than 9400 spectra of organic, polymeric, and inorganic materials. These spectra are compared to the unknown sample spectra using computer software to identify the “best match”. The changing in position of these phonon modes provided evidence of Sr atom in the unit cell. The FIC analysis shows that there is an inverse correlation between the superconductivity critical temperature T_c^{onset} and the crossover related to the fluctuations in the order parameter.

References

- Park C, Snyder RL (1995) Structures of high-temperature cuprate superconductors. J Am Ceram Soc 78: 3171-3194.
- Mattheiss LF (1990) Electronic structure and crystal chemistry of TlBa₂CuO₈ and related cuprate superconductors. Phys Rev B 42: 10108-10112.
- Maarit K, Yamauchi H (1999) The doping routes and distribution of holes in layered cuprates: a novel bond-valence approach. Philos Mag B 79: 343-366.
- Karppinen M, Yamauchi H, Morita Y, Kitabatake M, Motohashi T, et al. (2004) Hole concentration in the three-CuO₂-plane copper-oxide superconductor Cu-1223. J Solid State Chem 177: 1037-1043.
- Gang X, Xiong P, Cieplak MZ (1992) Universal hall effect in La_{1.85}Sr_{0.15}Cu_{1-x}A_xO₄ systems (A= Fe, Co, Ni, Zn, Ga). Phys Rev B 46: 8687.
- Gang X (1990) Magnetic pair-breaking effects: moment formation and critical doping level in superconducting La_{1.85}Sr_{0.15}Cu_{1-x}A_xO₄ systems (A=Fe, Co, Ni, Zn, Ga, Al). Phys Rev B 42: 8752.
- Mary TA, Kumar NRS, Varadaraju UV (1993) Influence of Cu-site substitution on the structure and superconducting properties of the NdBa₂Cu₃-xMxO_{7+δ} (M= Fe, Co) and NdBa₂Cu₃-xMxO_{7-δ} (M= Ni, Zn) systems. Phys Rev B 48: 16727.
- Awad R, Aly NS, Ibrahim IH, Abou-Aly AI, Saad AI (2000) Replacement study of Thallium by Zn and Ni in Tl-1223 superconductor phase. Physica C: Superconductivity 341: 685-686.
- Iyo A, Tanaka Y, Hirai M, Tokiwa K, Watanabe T (2003) Zn and Ni doping effect on anomalous suppression of T_c in an over doped region of TlBa₂Ca₂Cu₃O_{9-δ}. J Low Temp Phys 131: 643-646.
- Kuo YK, Schneider CW, Skove MJ, Nevitt MV, Tessema GX, et al. (1997) Effect of magnetic and nonmagnetic impurities (Ni, Zn) substitution for Cu in Bi₂(SrCa)_{2+n}(Cu_{1-x}M_x)_{1+n}O_y whiskers. Phys Rev B 56: 6201.
- Ibrahim EMM, Saleh SA (2007) Influence of sintering temperature on excess conductivity in Bi-2223 superconductors. Supercond Sci Technol 20: 672.
- Han SH, Axnäs J, Zhao BR, Rapp O (2004) Fluctuation conductivity at high temperatures in polycrystalline Hg, Tl-1223-Is there 1D fluctuation behavior? Physica C: Superconductivity 408: 679-680.
- Mumtaz M, Hasnain SM, AA Khurram, Nawazish A Khan (2011) Fluctuation induced conductivity in (Cu_{0.5}Tl_{0.5-x}K_x)Ba₂Ca₃Cu₄O_{12-δ} superconductor. J Appl Phys 109: 023906.
- Shun-Hui H, Lundqvist P, Rapp O (1997) Excess conductivity in Y_{1-x}Ca_xTbBa₂Cu₃O_{7-δ}. Physica C: Superconductivity 282: 1571-1572.
- Sato T, Nakane H, Yamazaki S, Mori N, Hirano S, et al. (2003) Analysis of fluctuation conductivity in melt-textured DyBa₂Cu₃O_y superconductors. Physica C: Superconductivity 392: 643-647.
- Felix V, Veira JA, Maza J, Garcia-Alvarado F, Moran E, et al. (1988) Excess electrical conductivity above T_c in high-temperature superconductors, and thermal fluctuations. Journal of Physics C: Solid State Physics 21: L599.
- Han SH, Eltsev Y, Rapp O (2000) Three-dimensional XY critical fluctuations of the dc electrical conductivity in Bi₂Sr₂CaCu₂O_{8+δ} single crystals. Phys Rev B 61: 11776.
- Ben Azzouz F, Zouaoui M, Annabi M, Ben Salem M (2006) Fluctuation conductivity analysis on the Bi-based superconductors processed under same conditions. Physica Status Solidi 3: 3048-3051.